

Published in final edited form as:

Angew Chem Int Ed Engl. 2014 July 1; 53(27): 7018–7022. doi:10.1002/anie.201400183.

A Facile Synthesis of Dynamic, Shape Changing Polymer Particles

Daniel Klinger,

Materials Research Laboratory, University of California, Santa Barbara, CA, 93106, USA

Cynthia Wang,

Materials Research Laboratory, University of California, Santa Barbara, CA, 93106, USA

Luke A. Connal,

Department of Chemical and Biomolecular Engineering University of Melbourne, Victoria 3010, Australia

Debra J. Audus,

Materials Research Laboratory, University of California, Santa Barbara, CA, 93106, USA

Se Gyu Jang,

Materials Research Laboratory, University of California, Santa Barbara, CA, 93106, USA

Stephan Kraemer,

Materials Research Laboratory, University of California, Santa Barbara, CA, 93106, USA

Kato L. Killops,

U.S. Army Edgewood Chemical Biological Center Aberdeen Proving Ground, MD, 21010, USA

Glenn H. Fredrickson,

Materials Research Laboratory, University of California, Santa Barbara, CA, 93106, USA

Edward J. Kramer, and

Materials Research Laboratory, University of California, Santa Barbara, CA, 93106, USA

Craig J. Hawker

Materials Research Laboratory, University of California, Santa Barbara, CA, 93106, USA

Craig J. Hawker: hawker@mrl.ucsb.edu

Abstract

We herein report a new facile strategy to ellipsoidal block copolymer nanoparticles exhibiting a pH-triggered anisotropic swelling profile. In a first step, elongated particles with an axially stacked lamellae structure are selectively prepared by utilizing functional surfactants to control the phase separation of symmetric PS-*b*-P2VP in dispersed droplets. In a second step, the dynamic shape change is realized by crosslinking the P2VP domains, hereby connecting glassy PS discs with pH-sensitive hydrogel actuators.

Keywords

shape anisotropy; block copolymers; nanoparticles; stimuli-responsive materials; microgels

The ability of nature to precisely control the shape and functionality of nanoparticles in a range of biological systems has long motivated researchers to strive for similar control in synthetic nanomaterials.^[1] This challenge has been partially fulfilled in inorganic systems where the ability to tailor shape and size in order to tune properties has been extensively studied.^[2] In direct contrast, the toolbox for controlling the shape and functionality of *polymer-based nanoparticles* is still in its infancy^[3] with future success being critical to the preparation of bio-inspired materials with applications ranging from drug-delivery systems to artificial camouflage.^[1c]

In addressing this need, the development of dynamic, shape-changing polymer particles requires three main structural features to be incorporated into a single system: shape anisotropy, spatial control over internal morphology and the introduction of stimuli-responsiveness to the nanoparticles. Unfortunately, current examples address each aspect separately with multifunctional, dynamic systems not being realized.^[3] Anisotropic particles, for instance, have been prepared by a multistep procedure which relies on the stretching of spherical particles.^[3a, 4] Even though such elongated particles show interesting properties^[5] only a few examples combine shape anisotropy with either well-defined internal morphologies^[6] or stimuli-responsive properties.^[7] For example, we have recently reported the use of tailored Au nanoparticles as surface active agents for the preparation of shape anisotropic particles with an internally structured morphology.^[8] While the potential of block copolymer self-assembly in colloidal systems is promising,^[9] the use of Au nanoparticles represents a significant synthetic limitation and did not lead to a dynamic, stimuli-responsive material. As a result, the facile formation of multifunctional nanoparticles that combine all three mentioned features (shape anisotropy, internal morphology, and stimuli-responsiveness) remains a major challenge.

Herein, we report the development of a facile and powerful new strategy for the preparation of functional particles that serves as a broad platform for nanoscale materials. Key to the success of this strategy is the use of functional surfactant mixtures to control the phase separation of symmetric PS-*b*-P2VP block copolymers (BCP) within dispersed nanoparticles. In analogy with the utilization of random copolymers in block copolymer lithography,^[10] mixtures of surfactants may allow for the accurate tuning of surface energies leading to selective switching between the three distinct internal morphologies shown in Scheme 1 with the final result being the controlled synthesis of spherical or elongated particles (Scheme 1). This approach further allows for secondary chemistry, such as crosslinking of the P2VP domains, to be achieved. These multifunctional particles not only combine an overall shape anisotropy with a well-defined internal morphology but also display a reversible pH-dependent swelling of the P2VP layers. Finally, the axially stacked internal lamellae morphology translates to an anisotropic swelling profile, thus resulting in a pH-triggered dynamic shape change due to a preferential stretching/shrinking of the elongated particles along the long axis.

The major initial challenge was the development of a method to control the phase separation of block copolymer building blocks in emulsion droplets. Traditionally, the use of a single surfactant or no surfactant at all, leads to an 'onion-like' radial morphology.^[11] This is due to preferential wetting of one block with the surfactant layer surrounding the dispersed particle. Such behaviour is in analogy with the selective wetting and associated self-assembly of BCPs in thin films. For thin films, the introduction of a neutral layer, typically a random copolymer, between the BCP and substrate and/or air can induce a perpendicular orientation of lamellae and cylinders.^[12] Our new approach to controlling the interaction between block copolymers and the surrounding medium is based on the concept of a neutral layer derived from a mixture of two surfactants. In this design, each surfactant would be preferential for one specific domain. Consequently, intermediate ratios of the two surfactants would lead to non-preferential interactions, in effect a neutral interface. In initial experiments with polystyrene-*b*-poly(2-vinyl pyridine) PS-*b*-P2VP and 100% cetyl trimethyl ammonium bromide (CTAB) as surfactant, the expected radial morphology was observed with polystyrene as the outermost layer due to hydrophobic interactions (Figure 1, Figure S-1a in SI). In designing a surfactant that would exhibit a preferential interaction with the P2VP phase, the ability of the 2VP groups to serve as hydrogen bond acceptors was exploited.^[13] A hydroxyl group was therefore incorporated at the ω -position of CTAB leading to HO-CTAB (see scheme 1).^[14] Significantly, the use of HO-CTAB resulted in the anticipated reverse behaviour and nanoparticles with P2VP as the outermost layer of an 'inverse onion' morphology (Figure 1, Figure S-1b) were obtained. This ability to switch the layer sequence by switching surfactants suggests that by adjusting the composition of the surfactant mixture, a neutral layer will be obtained. In analogy to the perpendicular orientation of lamellae in thin films, this neutral wetting behaviour will permit particles with the desired internal stacked lamellae structure to be obtained.

To test this hypothesis, a series of PS-*b*-P2VP (102k-97k) particles was prepared using mixtures of varying compositions of the two surfactants, whereby X is the mass fraction of HO-CTAB in relation to total surfactant concentration (see SI for experimental data). From the TEM images in Figure 1, it is demonstrated that tuning the mass fraction of surfactants is a facile technique to control both the self-assembly process and the particle shape. At high CTAB concentrations ($X = 0.50$), radial structures with a PS layer clearly at the surface are obtained. Significantly, as the mass fraction of HO-CTAB is increased above a 1:1 ratio ($X \sim 0.50$), a distinct morphology and shape change is observed to give spherical and non-spherical particles with a mixture of radially and axially stacked lamellae morphologies. A distinct transition is then observed at HO-CTAB concentrations, X, of between 0.70 and 0.80 where only the desired stacked lamellae morphology and ellipsoidal particle shape are observed. This confirms the validity of this mixed surfactant approach and the existence of a specific range of HO-CTAB/CTAB ratios for which the interfacial energies between the surfactants layer and the domains of the BCP are balanced. For the mid-point of the neutral range, $X = 0.75$, the interfacial balance results in *all* particles assuming an ellipsoidal shape with axially stacked lamella persistent throughout the entire particle (Figure 2). The simplicity and scalable nature of this strategy represents a modular synthetic technique for the preparation of nanostructured polymer ellipsoids.

Importantly, the aspect ratio of these shape anisotropic particles is not a fixed parameter since the elongation is determined by the counterbalance of three different contributions to the free energy. Theoretical calculations (see SI) indicate that, it is possible to shift this balance and thus tune the particle aspect ratio.^[8] To understand the effect of BCP molecular weight, three different lamellae forming PS-*b*-P2VP diblock copolymers were examined – 102k-97k, 40.5k-41k, and 20k-20k. By plotting both theoretical and experimental aspect ratio (A) vs. the long axis (L) of ellipsoidal particles (formed from a HO-CTAB/CTAB ratio of 3:1, i.e. $X = 0.75$) (see Figure 3b) it is evident that elongation not only increases with block copolymer molecular weight but also with particle size. Regarding the latter, the theoretical model predicts that larger droplets/particles are easier to stretch since the droplet surface energy decreases in relation to the bulk elastic and interfacial free energy contributions with increasing particle size (see SI). This strong influence of droplet volume on elongation is demonstrated by an increase in aspect ratio with particle size as shown in the plots in Figure 3b. Regarding the influence of the BCP molecular weight, the theoretical model predicts that it is easier to stretch particles consisting of BCPs with higher molecular weights since the energetic penalty for the chain stretching is higher for shorter polymers. This assumption is strongly supported by the results in Figure 3 where decreasing the overall MW of symmetrical PS-*b*-P2VP block copolymers decreases the aspect ratio of the colloids. As shown in Figure 3, TEM images of similarly sized particles (ca. 550 nm in length) demonstrate that different aspect ratios are obtained for similar L values and a direct correlation between the number of layers per particle and molecular weight is obtained.

Having demonstrated the ability to tune shape and internal morphology, introduction of stimuli-responsiveness was investigated by taking advantage of the nucleophilicity and basic character of the 2VP units present in the PS-*b*-P2VP block copolymer. In order to render the ellipsoidal particles pH responsive while maintaining their integrity, the P2VP chains were crosslinked by the addition of 1,4-dibromobutane (DBB), transforming the P2VP domains into hydrogel materials.^[15] Significantly, crosslinking did not change the internal morphology or shape of the particles at neutral pH (Figure 4a). However, upon lowering the pH, the remaining 2VP units are protonated, causing the P2VP hydrogel layers to undergo significant swelling. As these hydrogel layers are connected by glassy PS lamellae, the swelling results in a dramatic elongation of the ellipsoids along the long axis L . Particles with 8 lamellae swell from around 550 nm at pH 7 to approximately 1400 nm at pH 3 with TEM analysis showing a unique shape change from ellipsoidal to an ‘accordion-like’, segmented structure (Figure 4a). Since the short axis (D) of the particles remains unaltered this pH-induced shape change corresponds to a more than 250% increase in the aspect ratio. Of even greater importance is the observation that these dramatic changes are reversible, by increasing the pH from 3 to 10, the initial stacked lamellae structure and ellipsoidal shape of the elongated particles is fully restored (Figure 4a). In direct contrast, non-crosslinked materials do not undergo reversible switching or dramatic shape changes. Under acidic conditions (pH < 4.5) complete disintegration of the ellipsoid particles into glassy PS nano-discs with P2VP coronas occurs (Figure 4b). All attempts to reverse this process by increasing the pH failed with clusters of nano-discs remaining. In addition, attempts to exploit responsive properties for the spherical, radial lamella structures, either before or after crosslinking, did not lead to any shape or morphology changes. The reversible shape

transformation for the ellipsoidal, stacked lamella particles therefore represents a unique platform that is enabled by the ability to control crosslinking, shape and morphology in a single system.

In summary, we have demonstrated a facile method to control particle shape and morphology through the use of tailored, mixed surfactant systems to tune surface interactions. For PS-*b*-P2VP particles, three disparate morphologies: spherical particles consisting of radial layers with either PS or P2VP as the outer layer and ellipsoidal particles containing axially stacked lamellae could be reproducibly and exclusively obtained. In addition, by adjusting the molecular weight of the block copolymer, control over the aspect ratio and therefore the shape anisotropy of these prolate ellipsoids could be realized. In an interesting demonstration of the interplay between chemistry, surface interactions and nanoscale morphology, crosslinking of the P2VP domains allows the pH-responsiveness of the 2VP moieties to be exploited leading to shape and structure- responsive particles. The simplicity and generality of this synthetic strategy allows access to novel, shape anisotropic and responsive polymer particles with applications ranging from colloidal self-assembly to photonics and biomedical delivery devices.

Supplementary Material

Refer to Web version on PubMed Central for supplementary material.

Acknowledgments

This work was supported by the MRSEC Program of the National Science Foundation (NSF) under Award DMR-1121053 (LAC, DJA, SK, EJK and CJH), the Institute for Collaborative Biotechnologies through grant W911NF-09-0001 from the U.S. Army Research Office (DK, SGJ, KKK, GHF, CJH) and the National Heart, Lung, and Blood Institute, National Institutes of Health, Department of Health and Human Services, under Contract No. HHSN268201000046C (DK, CW, CJH). Facilities support from the CNSI-MRL Center for Scientific Computing (DMR-1121053 and CNS-0960316). The content of the information does not necessarily reflect the position or the policy of the US government and no official endorsement should be inferred.

References

1. (a) Ballauff M, Lu Y. *Polymer*. 2007; 48:1815–1823. (b) Dugyala VR, Daware SV, Basavaraj MG. *Soft Matter*. 2013; 9:6711–6725. (c) Champion JA, Mitragotri S. *Proc. Natl. Acad. Sci. USA*. 2006; 103:4930–4934. [PubMed: 16549762] (d) Nayak S, Lyon LA. *Angew. Chem. Int. Ed*. 2005; 44:7686–7708.
2. (a) Sau TK, Rogach AL. *Adv. Mater*. 2010; 22:1781–1804. [PubMed: 20512953] (b) Gou LF, Murphy CJ. *Chem. Mater*. 2005; 17:3668–3672.
3. (a) Champion JA, Katare YK, Mitragotri S. *Proc. Natl. Acad. Sci. USA*. 2007; 104:11901–11904. [PubMed: 17620615] (b) Motornov M, Roiter Y, Tokarev I, Minko S. *Prog. Polym. Sci*. 2010; 35:174–211. (c) Perry JL, Herlihy KP, Napier ME, Desimone JM. *Acc. Chem. Res*. 2011; 44:990–998. [PubMed: 21809808] (d) Yabu H, Higuchi T, Shimomura M. *Adv. Mater*. 2005; 17:2062–2065.
4. Ho CC, Keller A, Odell JA, Ottewill RH. *Colloid. Polym. Sci*. 1993; 271:469–479.
5. Yunker PJ, Still T, Lohr MA, Yodh AG. *Nature*. 2011; 476:308–311. [PubMed: 21850105]
6. (a) Jeon SJ, Yi GR, Yang SM. *Adv. Mater*. 2008; 20:4103–4108. (b) Mei SL, Wang L, Feng XD, Jin ZX. *Langmuir*. 2013; 29:4640–4646. [PubMed: 23506093] (c) Deng RH, Liang FX, Li WK, Liu SQ, Liang RJ, Cai ML, Yang ZZ, Zhu JT. *Small*. 2013; 9:4099–4103. [PubMed: 23554338] (d) Deng RH, Liang FX, Li WK, Yang ZZ, Zhu JT. *Macromolecules*. 2013; 46:7012–7017.

7. (a) Ohm C, Kapernaum N, Nonnenmacher D, Giesselmann F, Serra C, Zentel R. *J. Am. Chem. Soc.* 2011; 133:5305–5311. [PubMed: 21413762] (b) Yoo JW, Mitragotri S. *Proc. Natl. Acad. Sci. USA.* 2010; 107:11205–11210. [PubMed: 20547873]
8. Jang SG, Audus DJ, Klinger D, Krogstad DV, Kim BJ, Cameron A, Kim SW, Delaney KT, Hur SM, Killips KL, Fredrickson GH, Kramer EJ, Hawker CJ. *J. Am. Chem. Soc.* 2013; 135:6649–6657. [PubMed: 23594106]
9. (a) Higuchi T, Motoyoshi K, Sugimori H, Jinnai H, Yabu H, Shimomura M. *Soft Matter.* 2012; 8:3791–3797. (b) Higuchi T, Tajima A, Motoyoshi K, Yabu H, Shimomura M. *Angew. Chem. Int. Ed.* 2008; 47:8044–8046. (c) Jeon SJ, Yi GR, Koo CM, Yang SM. *Macromolecules.* 2007; 40:8430–8439. (d) Li L, Matsunaga K, Zhu JT, Higuchi T, Yabu H, Shimomura M, Jinnai H, Hayward RC, Russell TP. *Macromolecules.* 2010; 43:7807–7812.
10. (a) Sweat DP, Kim M, Yu X, Schmitt SK, Han E, Choi JW, Gopalan P. *Langmuir.* 2013; 29:12858–12865. [PubMed: 24053350] (b) Xu J, Russell TP, Checco A. *Small.* 2013; 9:779–784. [PubMed: 23180675]
11. (a) Higuchi T, Shimomura M, Yabu H. *Macromolecules.* 2013; 46:4064–4068. (b) Higuchi T, Tajima A, Motoyoshi K, Yabu H, Shimomura M. *Angew. Chem. Int. Ed.* 2009; 48:5125–5128. (c) Higuchi T, Yabu H, Onoue S, Kunitake T, Shimomura M. *Colloids Surf., A.* 2008; 313:87–90. (d) Yabu H, Higuchi T, Shimomura M. *Adv. Mater.* 2005; 17:2062–2065.
12. (a) Bates CM, Seshimo T, Maher MJ, Durand WJ, Cushen JD, Dean LM, Blachut G, Ellison CJ, Willson CG. *Science.* 2012; 338:775–779. [PubMed: 23139327] (b) Son JG, Bulliard X, Kang HM, Nealey PF, Char K. *Adv. Mater.* 2008; 20:3643–3648. (c) Huang E, Pruzinsky S, Russell TP, Mays J, Hawker CJ. *Macromolecules.* 1999; 32:5299–5303. (d) Ji S, Liu CC, Son JG, Gotrik K, Craig GSW, Gopalan P, Himpel FJ, Char K, Nealey PF. *Macromolecules.* 2008; 41:9098–9103. (e) Mansky P, Liu Y, Huang E, Russell TP, Hawker CJ. *Science.* 1997; 275:1458–1460.
13. (a) Deng RH, Liu SQ, Li JY, Liao YG, Tao J, Zhu JT. *Adv. Mater.* 2012; 24:1889–1893. [PubMed: 22407538] (b) Klinger D, Robb MJ, Spruell JM, Lynd NA, Hawker CJ, Connal LA. *Polymer Chemistry.* 2013; 4:5038–5042. (c) van Zoelen W, Asumaa T, Ruokolainen J, Ikkala O, ten Brinke G. *Macromolecules.* 2008; 41:3199–3208. (d) Li QF, He JB, Glogowski E, Li XF, Wang J, Emrick T, Russell TP. *Adv. Mater.* 2008; 20:1462–1466. (e) Heo K, Miesch C, Emrick T, Hayward RC. *Nano Lett.* 2013; 13:5297–5302. [PubMed: 24164466] (f) An ZS, Shi Q, Tang W, Tsung CK, Hawker CJ, Stucky GD. *J. Am. Chem. Soc.* 2007; 129:14493–14499. [PubMed: 17967023] (g) Park N, Seo M, Kim SY. *J. Polym. Sci., Part A, Polym. Chem.* 2012; 50:4408–4414.
14. Davey TW, Ducker WA, Hayman AR. *Langmuir.* 2000; 16:2430–2435.
15. (a) Cheng L, Hou GL, Miao JJ, Chen DY, Jiang M, Zhu L. *Macromolecules.* 2008; 41:8159–8166. (b) Hui TR, Chen DY, Jiang M. *Macromolecules.* 2005; 38:5834–5837. (c) Kang Y, Walish JJ, Gorishnyy T, Thomas EL. *Nature Materials.* 2007; 6:957–960. (d) Thurmond KB, Kowalewski T, Wooley KL. *J. Am. Chem. Soc.* 1996; 118:7239–7240. (e) Thurmond KB, Kowalewski T, Wooley KL. *J. Am. Chem. Soc.* 1997; 119:6656–6665.

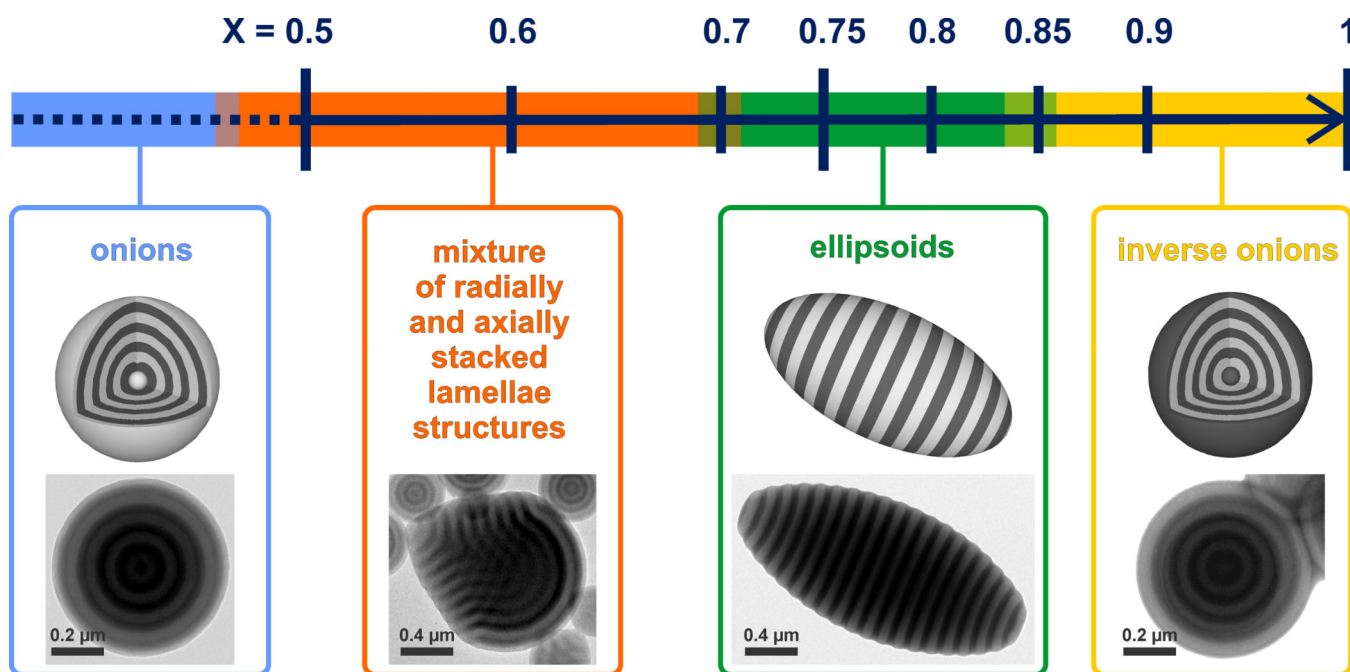


Figure 1. Schematic representation of the influence of the mass fraction (X) of HO-CTAB – in a binary mixture with CTAB – on the shape and internal morphology of particles formed from a PS-*b*-P2VP (102k-97k) diblock copolymer (representative TEMs are provided for each distinct morphological region).

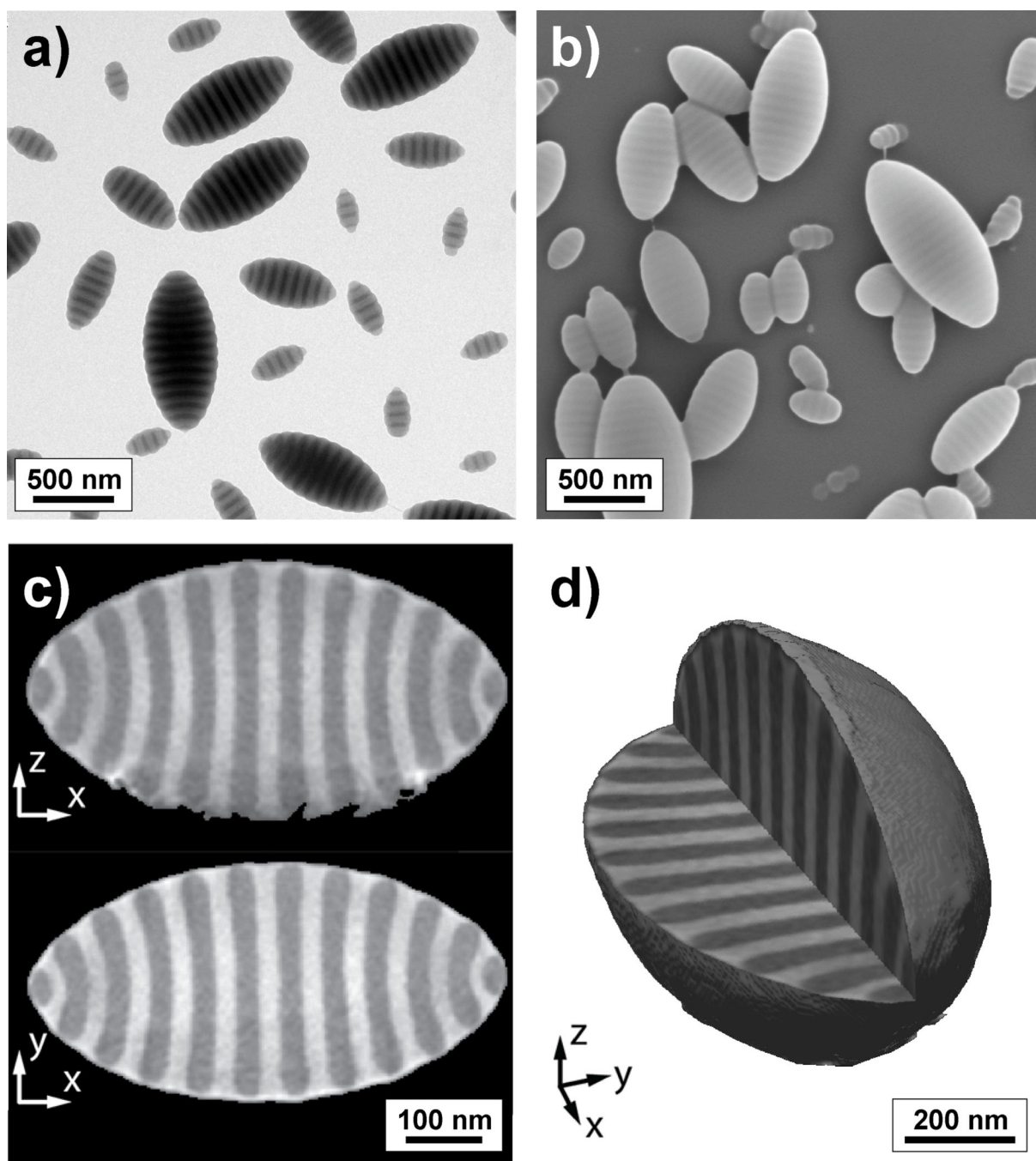


Figure 2. Electron micrographs of the prolate ellipsoids with axially stacked lamellae obtained via the solvent evaporation-driven self-assembly of PS-*b*-P2VP (102k-97k) from CHCl₃ droplets emulsified with a mixture of surfactants, X(HO-CTAB) = 0.75: a) TEM, b) SEM, c) TEM slices extracted from the full 3D reconstructed image and d) reconstructed 3D image from TEM tomography.

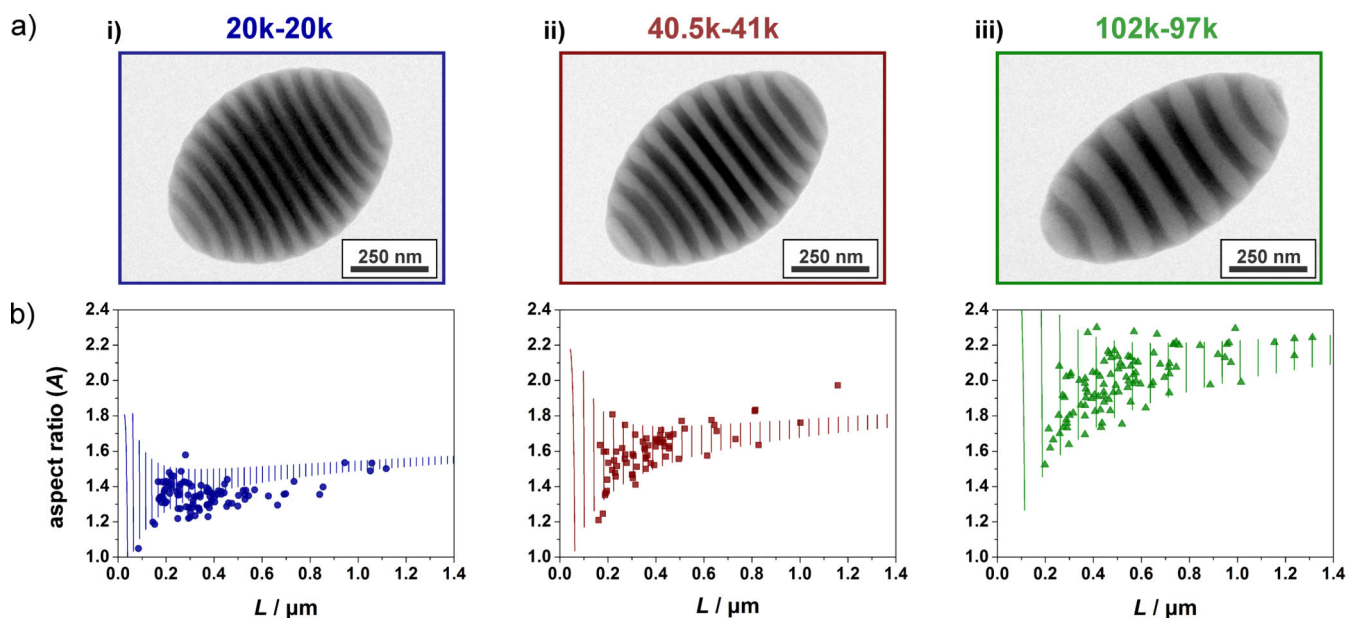
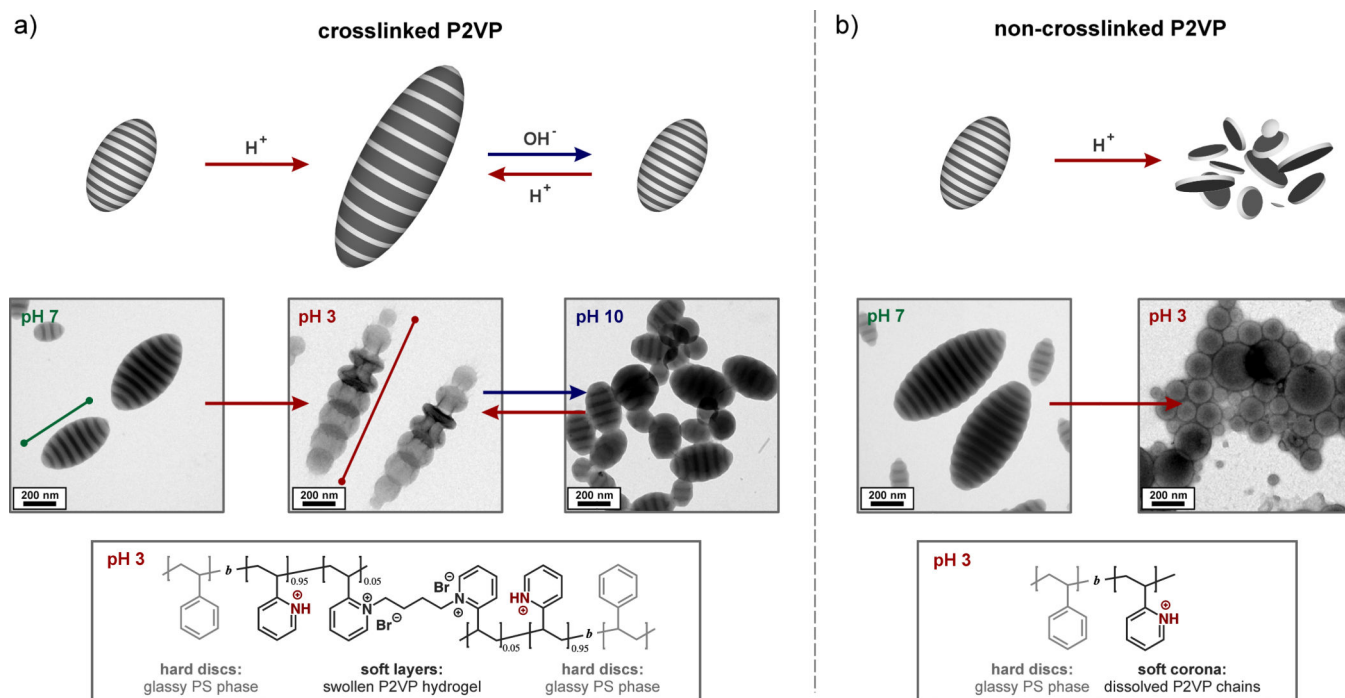
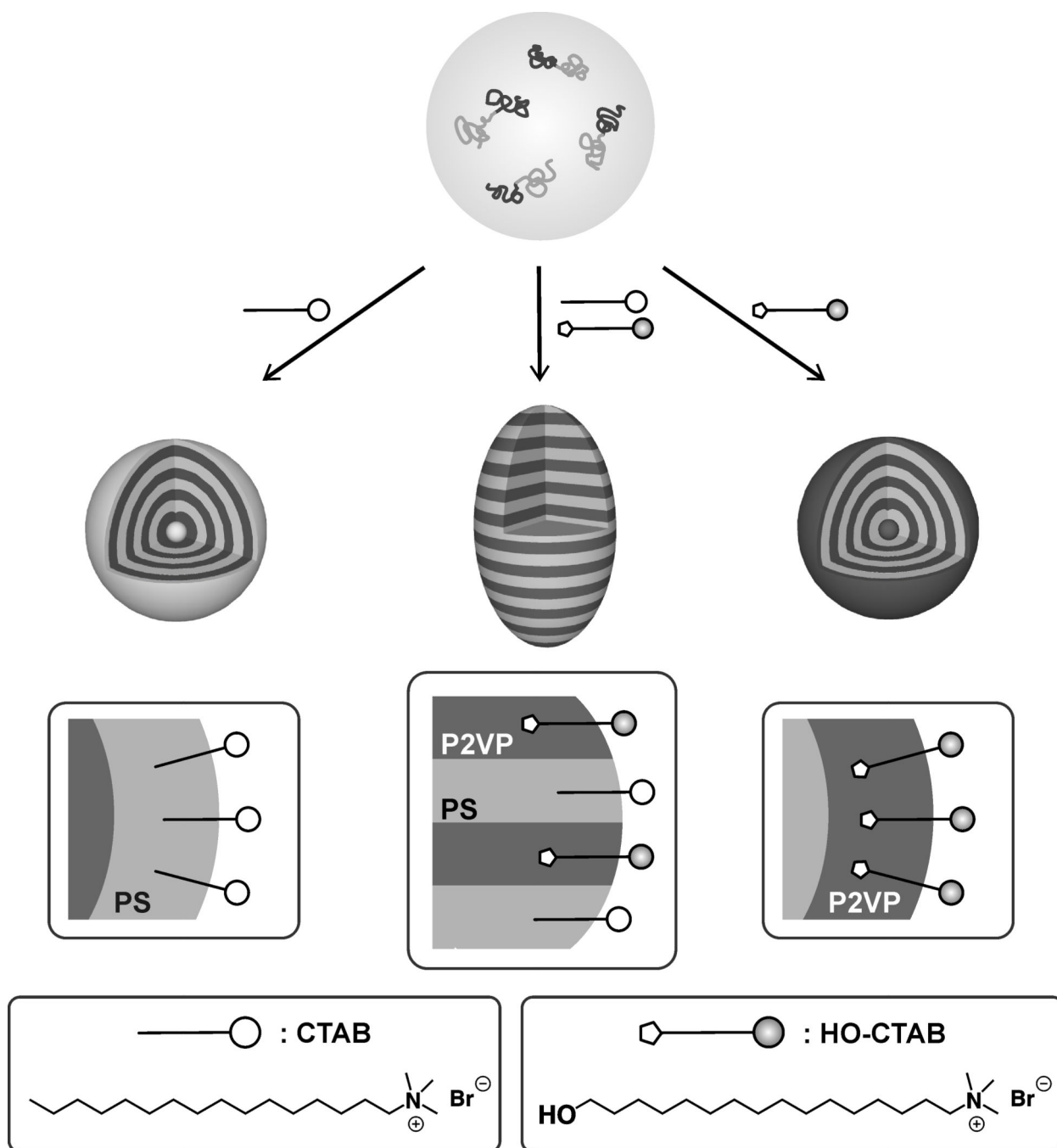


Figure 3.

Influence of BCP molecular weight on the shape anisotropy of ellipsoidal PS-*b*-P2VP nanoparticles with axially stacked lamellae obtained for neutral wetting conditions 3:1 ratio of HO-CTAB:CTAB ($X=0.75$): a) TEM images of similar sized ($L \sim 550$ nm) BCP nanoparticles obtained from PS-*b*-P2VP diblock copolymers with molecular weights of (i) 20k-20k, (ii) 40.5k-41k and (iii) 102k-97k; b) Plots of experimental (● dots) and theoretically (—lines) predicted aspect ratios (L/D) in dependency on the long axis (L) for representative populations of the 3 respective diblock copolymer molecular weights.

**Figure 4.**

Investigations on the pH-responsive behavior of PS-*b*-P2VP ellipsoidal particles with axially stacked lamellae: a) pH-triggered dynamic shape change for particles with crosslinked (5 mol-% 1,4-dibromobutane) P2VP domains due to swelling/deswelling of the P2VP-based hydrogel discs. The demonstrated variation of the aspect ratio was fully reversible for at least three cycles; b) discrete nanodiscs were obtained for non-crosslinked systems due to solubilization of P2VP chains.

**Scheme 1.**

Schematic representation of a mixed surfactant strategy for controlling the self-assembly of PS-*b*-P2VP and the generation of particles with defined shape and internal morphology via solvent evaporation from droplets.